A Unified Global Self-Consistent Model of a Capacitively and Inductively Coupled Plasma Etching System

Yoon-Bong Hahn† and Stephen J. Pearton*

School of Chemical Engineering and Technology, Chonbuk National University,
Chonju 561-756, Korea
*Department of Materials Science and Engineering, University of Florida,
Gainesville, FL 32611, USA
(*Received 5 October 1999 • accepted 24 January 2000*)

Abstract−Based on the concept of independent control of ion flux and ion-bombardment energy, a global self-consistent model was proposed for etching in a high-density plasma reactor. This model takes account of the effect on the plasma behavior of separate rf chuck power in an Inductively Coupled Plasma etching system. Model predictions showed that the chuck power controls the ion bombardment energy but also slightly increases the ion density entering the sheath layer, resulting in an increase in etch rate (or etch yield) with increasing this rf chuck power. The contribution of the capacitive discharge to total ion flux in the ICP etching process is less than about 6% at rf chuck powers lower than 250 W. As a model system, etching of InN was investigated. The etch yield increased monotonically with increasing the rf chuck power, and was substantially affected by the ICP source power and pressure. The ion flux increased monotonically with increasing the source power, while the dc-bias voltage showed the reverse trend.

Key words: Global Self-consistent Model, Inductively Coupled Plasma, ICP Etching

INTRODUCTION

Inductively Coupled Plasma (ICP) etching is an effective high density plasma technique for patterning of III-V and III-nitride materials [Shul et al., 1996, 1997; Pearton et al., 1994, 1998, 1999; Hahn et al., 1999]. The ICP plasmas are formed in a dielectric vessel encircled by an inductive coil into which rf power is applied (see Fig. 1(a)). The rf current circulating around the chamber causes an alternating magnetic field in upward and downward directions. The change in rate of the magnetic field then induces an rf electric field. This rf field will accelerate the electrons into a circular path, confining them in a circular motion. The power transfer through the dielectric window by inductive coupling is efficient, leading to high ion density. As long as the capacitively coupled component is absent or at least small, the electrons trapped in a circular path will have only a small chance to be lost to the substrate electrode, resulting in low dc bias.

Since the ion energy and plasma density can be effectively decoupled, uniform density and energy distributions are transferred to the sample. However, the ion-bombarding energy under these conditions is often too low to initiate etching because the high density discharges have low-voltage (20-40 V) sheaths near almost all surfaces. To control the ion energy, the sample chuck (i.e., substrate electrode) is independently driven by a capacitively coupled rf source, leading to anisotropic etching. ICP sources are generally believed to have several advantages over Electron Cyclotron Resonance (ECR) sources: 1) easier scale-up of source for production applications, 2) improved plasma uniformity over a wide area, and 3) lower cost of ownership.

In recent years, associated with increasing interest in the ICP etching systems for semiconductor and related processing, mathematical modeling has been used to understand the fundamental aspects of the low pressure plasma behavior. Most of the modeling studies include one-dimensional fluid models or Monte Carlo techniques [Liberman et al., 1993, 1994; Stewart et al., 1994; Wu et al., 1997], and two-dimensional fluid models

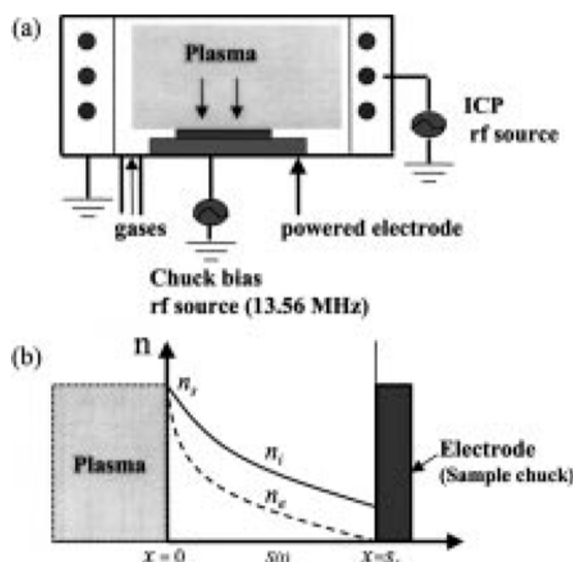

Fig. 1. Schematic illustrations of (a) ICP etching system and (b) ion densities in the sheath region in contact with the wall of a sample chuck.

†To whom correspondence should be addressed.
E-mail: ybhahn@chonbuk.ac.kr

[Economou et al., 1995; Bukowski, 1996; Collision and Kushner, 1996; Rauf and Kushner, 1997]. It has been found that the two-dimensional fluid models produce better predictions of the bulk plasma behavior than the one-dimensional ones. Most of these simulation works have focused on better understanding of bulk plasma behavior, and on investigating the effects of reactor design and operating conditions on plasma uniformity and energy and angular distributions. However, current mathematical models are generally not able to properly include the effects of collisionless heating and the capacitive discharge formed by rf power applied to a sample chuck, especially for ICP systems. Furthermore, little work has been reported on the effects of operating conditions on etch yield.

In this work, as a partial fulfillment of the overall project of modeling the ICP etching system, a global self-consistent model was developed to take account of the effect of the capacitive discharge coupled by the rf chuck power and the stochastic heating within the sheath layer. In this model, the ICP system was assumed as a combined system of the inductive coupled discharge plus the capacitive discharge. It was also designed to provide process engineers with a simple but reasonably accurate model so that they can easily calculate plasma parameters and utilize the results to optimize the etching conditions and possible system redesigns. The model can give relatively accurate predictions of plasma behavior under various conditions.

MODEL EQUATIONS

Since the quasi-independent control of the ion flux through the source power and the ion bombardment energy through the chuck power is possible, the ICP etching system can be considered as a combined plasma system by capacitive and inductive coupled discharges:

$$[\text{ICP System}]=[\text{Inductive Coupled Discharge}]+[\text{Capacitive Discharge}] \tag{1}$$

Eq. (1) is a conceptual frame of the global self-consistent model used in this work for a cylindrical ICP etching system shown in Fig. 1(a).

We have the following assumptions for the ICP system having a cylindrical geometry:

(1) A uniform cylindrical plasma is assumed for the inductive coupled discharge, and Maxwellian electrons absorb the electrical power supplied through an inductive coil. This is generally acceptable because at high density a plasma's electron-electron collisions change the electron distribution function to Maxwellian form [Liberman and Lichtenberg, 1994; Kortshagen et al., 1995].

(2) For the capacitive discharge, the ions respond only to the time-averaged potentials, while the electrons respond to the instantaneous potentials and carry the rf discharge current. The plasma and the sheath are allowed to be inhomogeneous.

(3) The electron density is zero within the sheath regions, and the ions enter the sheath with the Bohm velocity.

(4) The voltage across the sheath in the inductive discharge is much smaller than that in the capacitive discharge. This is generally true, and leads to an assumption that the stochastic heating in the ICP etching system is mainly attributed to the rf power applied to the sample chuck.

1. Inductive Coupled Discharge

A global model developed for bulk plasma in an ICP system by Lieberman et al. [1993, 1994] has been found useful to predict plasma parameters for low pressure, high density plasmas. The model predicts electron temperature by equating the total volume ionization rate to the surface ion (or particle) loss rate. Since the ion-electron pairs are created primarily by electron-neutral ionization, the plasma density is not directly affected by other subprocesses. If the electron-neutral ionization rate is constant in the bulk of the plasma, based on the conservation law the global particle balance is expressed as:

$$K_{iz}N_g n_o V_R=\Gamma_{tb}+\Gamma_s=n_o u_B(2\pi R^2 h_L+2\pi RLh_R) \tag{2}$$

where K_{iz}, N_g, n_o, V_R, Γ_{tb}, Γ_s and u_B represent the ionization rate constant, neutral gas density, plasma density, reactor volume, the ion flux on the top and bottom walls, ion flux on side wall, and the Bohm velocity, respectively. L, R, h_L and h_R are the discharge length, cylindrical radius, axial and radial ratios of center-to-edge ion density, respectively. Eq. (2) can be rewritten as

$$\frac{K_{iz}(T_e)}{u_B(T_e)}=\frac{\Gamma}{u_B N_g n_o V_R}=\frac{1}{N_g d_{eff}} \tag{3}$$

where

$$d_{eff}=\frac{RL}{2(Rh_L+Lh_R)} \tag{4}$$

$$h_L=\frac{n_{sL}}{n_o}\approx 0.86\left(3+\frac{L}{2\lambda_i}\right)^{-1/2} \tag{5}$$

$$h_R=\frac{n_{sR}}{n_o}\approx 0.8\left(4+\frac{R}{\lambda_i}\right)^{-1/2} \tag{6}$$

$$\lambda_i=\frac{1}{\sigma N_g} \tag{7}$$

where σ, n_{sL} and n_{sR} are the cross section for momentum transfer between ions and neutrals, and ion densities at the axial edge and at the radial edge of the sheath, respectively. Eq. (3) indicates that the electron temperature is determined by the ion-neutral mean-free path (λ_i), not by the electron energy balance. Hence, the effect of gas pressure is incorporated by means of an effective plasma size (d_{eff}) that is a function of a mean-free path. The ionization rate constant is a function of electron temperature and can be expressed as an Arrhenius form [Lieberman et al., 1993, 1994; Wu et al., 1997]:

$$K_{iz}=k_o\bar{u}_e\exp\left(\frac{-\varepsilon_{iz}}{T_e}\right) \tag{8}$$

where k_o, $\bar{u}_e$ and ε_{iz} are a constant, electron mean thermal speed $[(8T_e/\pi m_e)^{1/2}]$, and ionization energy, respectively.

The total energy loss per electron-ion pair in the system is given:

$$\varepsilon_t=\varepsilon_c+\varepsilon_k+\varepsilon_i \tag{9}$$

where ε_c, ε_k and ε_i represent the collisional energy loss per electron-ion pair, the mean kinetic energy lost per electron, and

the ion bombardment energy (or the mean kinetic energy lost per ion), respectively, and they are given by [Liberman et al., 1993, 1994; Stewart et al., 1994].

$$\varepsilon_c=\varepsilon_{iz}+\frac{K_{ex}\varepsilon_{ex}+3K_{el}(m/T)T_e}{K_{iz}} \quad (10)$$

$$\varepsilon_{iz}=(3m/M)T_e \quad (11)$$

$$\varepsilon_k=2T_e \quad (12)$$

$$\varepsilon_i=\frac{T_s}{2}\left[1+\ln\left(\frac{M}{2\pi m}\right)\right] \quad (13)$$

The overall global power balance for the inductive coupled discharge is written as

$$P_{a,icp}=eu_B n_o A_{eff}\varepsilon_T \quad (14)$$

where $P_{a,icp}$ and A_{eff} are the power absorbed in the plasma and an effective area of plasma, respectively. Eq. (14) can be used to calculate the ion density of the inductively coupled discharge.

The sheath thickness formed by the inductive discharges can be obtained by

$$s_{t,icp}=\left(\frac{0.82\varepsilon_o}{en_s u_B}\right)^2\left(\frac{2e}{M}\right)\frac{V_{rf}^3}{(r_c-R)^3} \quad (15)$$

where (r_c-R) is the thickness of the dielectric interface separating coil and plasma, r_c is the radius of the inductive coils, and V_{rf} is the voltage of ICP rf source.

2. Capacitive Discharge

Since the sample chuck is capacitively driven by an additional rf power supply in order to increase the ion bombardment energy, a capacitive discharge is also formed in the ICP system. The voltage across the sheath in the capacitive discharge is much larger than that in the inductive discharge, and in turn the stochastic heating within the inhomogeneous sheath becomes more significant. Furthermore, the decreasing ion density within the sheath leads to a Child law variation of the density, an increased sheath width, and an increase of the sheath velocity [Lieberman and Lichtenberg, 1994]. The increase in sheath width decreases the total sheath capacitance. Hence, a self-consistent model must account for all of these effects together and consider collisionless sheath dynamics. The structure of the rf sheath is illustrated in Fig. 1(b). Ions crossing the ion sheath boundary at x=0 accelerate within the sheath strike the electrode at $x=S_t$.

In the capacitive discharge system, the power transfer mechanism consists of ohmic heating (the power transferred to the electrons due to collisional momentum transfer between electrons and neutrals in the bulk) and stochastic heating (the power transferred to the electrons within the sheath). Details of all of these are described elsewhere [Lieberman and Lichtenberg, 1994]. Since the mean free path of ions is greater than plasma radius in the ICP system (i.e., $\lambda_i \geq (T_i/T_e)d$), the electron ohmic heating power per unit area is given by

$$\overline{P}_{ohm}\approx 1.73\frac{m}{2e}\left(\frac{n_s}{n_o}\right)\varepsilon_o\omega^2 v_m (T_e V_1)^{1/2} d, \quad (16)$$

The stochastic heating power is given by

$$\overline{P}_{stoc}\approx 0.45\left(\frac{m}{2e}\right)^{1/2}\varepsilon_o\omega^2 T_e^{1/2} V_1 \quad (17)$$

In Eqs. (16) and (17), ω represents the radian frequency of a capacitive plasma source, V_1 is the sheath potential, and d is the plasma size and approximated as $d=L-2s_m$. The sheath thickness (s_m) formed by the capacitive discharge can be obtained by the Child law for the self-consistent ion sheath, which is obtained by integrating the Poisson equation for the instantaneous electric field within the sheath layer.

The electron power balance equation for the capacitive discharge is then obtained by

$$P_e=\overline{P}_{ohm}+2\overline{P}_{stoc}=2en_s u_s(\varepsilon_c+2T_e) \quad (18)$$

It is worthwhile to note that the ohmic heating power can be neglected if the reactor pressure is sufficiently low. Since $u_s=u_B$ for a collisionless sheath, the ion flux at the sheath edge can be calculated from Eq. (18). The total power absorbed per unit area for the capacitive discharge is then found as

$$P_{a,ccp}=2en_s u_B(\varepsilon_c+\varepsilon_i+2T_e) \quad (19)$$

where, neglecting the voltage drop across the bulk plasma, $\varepsilon_i=\overline{V}\approx 0.42V_{rf}\approx 0.83V_1$. V_{rf} is the rf voltage applied to the sample chuck. Combining Eqs. (18) and (19), we find

$$P_{a,ccp}=P_e\left(1+\frac{0.83V_1}{\varepsilon_c+2T_e}\right) \quad (20)$$

Hence, the total power absorbed in the ICP system can be obtained by summing Eqs. (14) and (20).

Using Eqs. (1), (5), (14) and (18), we obtain the overall ion density and ion flux at the sheath edge in the ICP etching system

$$n_s=n_{s,icp}+n_{s,ccp}=h_L n_o+\frac{\overline{P}_{ohm}+2\overline{P}_{stoc}}{2eu_B(\varepsilon_c+2T_e)} \quad (21)$$

$$\Gamma_i=\Gamma_{i,icp}+\Gamma_{i,ccp}=n_s u_B \quad (22)$$

It is worth noting that Eqs. (1), (21) and (22) can be used for the reactive ion etching (RIE) system by setting $n_{s,icp}=0$ and $G_{i,icp}=0$.

3. Etch Yield

Etch yield can be defined as number of atoms etched per incident ion and expressed as:

$$Y=\frac{R_{E,atom}}{\Gamma_i}=\frac{r_E\rho_s NA}{\Gamma_i M_s} \quad (23)$$

where r_E, ρ_s, M_s, N and A represent etch rate, density and molecular weight of the material to be etched, Avogadro number and number of atoms per one molecule of the substrate, respectively. The etch yield is then calculated given etch rate with the ion flux at the sheath edge obtained from Eq. (22).

RESULTS AND DISCUSSION

Model predictions were made for an argon discharge in an ICP system (R=15 cm and L=6 cm), and compared with those obtained by Stewart et al. [1994] using a two-dimensional fluid model. The results are shown in Fig. 2 in terms of electron temperature and plasma density with varying pressure and ICP

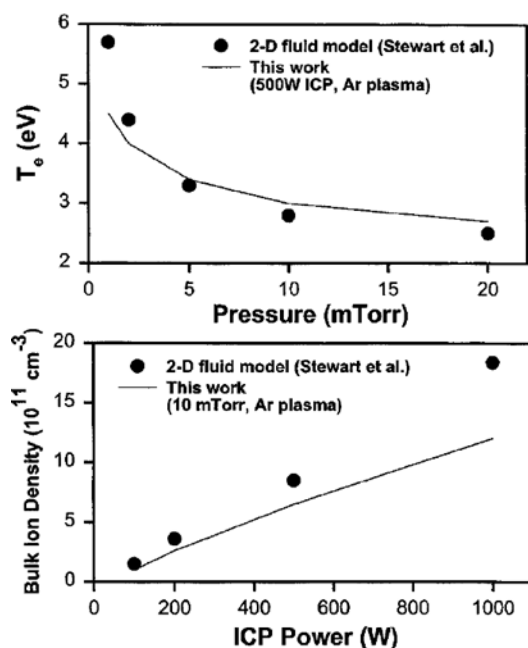

Fig. 2. Effects of pressure (top) and ICP source power (bottom) on electron temperature and plasma density, respectively.

source power. Relatively good agreement between the two models was obtained, showing that the electron temperature was less dependent on neutral gas pressure at higher pressures (Fig. 2, top). Although not illustrated, the electron temperature was independent of the ICP source power, indicating that it is only a function of the ion-neutral mean free path or the reactor pressure. The plasma density at the center of the discharge showed a linear relationship with the ICP source power for both models (bottom). The quantitative difference between the two models is attributed to several reasons: (1) approximate expression of $d_{eff}(\lambda_i)$ and $A_{eff}(\lambda_i)$ for the global self-consistent model, (2) approximation of the plasma potential in the two-dimensional fluid model (that is, peak potential minus 0.5 T_e), and (3) rough grid points used in the fluid model predictions. However, both models showed overall good agreement and the same trend, indicating that the electron temperature and the plasma density are mainly determined by the ion continuity equation and the power balance equation, respectively. This comparison leads to the conclusion that the global self-consistent model in this work can be used for predicting the plasma parameters in the ICP system with less computational cost.

The global models developed previously did not take into account the effect of capacitive discharge, leading to an independence of the ion flux on the chuck power. However, the global self-consistent model proposed in this work includes its effect. Fig. 3 shows the effect of the rf chuck power on the ion density at the sheath edge for the argon ICP discharge. It is seen that the ion flux increases substantially with increasing rf power (denoted by ○), while that in the counterpart by the inductively coupled discharge maintains a constant value (denoted by ●). Hence the model predictions lead to a conclusion that the rf chuck power increases not only the ion bombardment

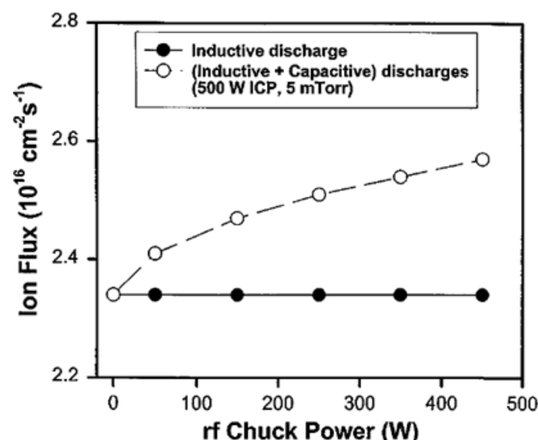

Fig. 3. Effect of rf chuck power on ion flux at the sheath edge (500 W ICP, 5 mTorr, Ar plasma).

energy but also the ion density entering the sheath layer, resulting in an increase in etch rate (or etch yield) with increasing the chuck power. However, the contribution of the capacitive discharge to total ion flux in the ICP etching process is less than about 6% at rf powers lower than 250 W, indicating that the main role of the chuck power is to increase the ion bombarding energy.

Model predictions were also carried out for the ICP etching of InN in ICl/Ar plasmas in terms of etch yield and ion flux at the sheath edge with varying the ICP source power, rf chuck power and pressure. The InN samples were etched in a Plasma-Therm ICP system (R=20 cm, L=18 cm). The ICP power, rf chuck power and pressure were varied between 0-750 W, 50-350, and 5-20 mTorr, respectively. The predicted results of etch yield and ion flux together with measured dc-bias voltages are shown in Figs. 4-6. Here, the etch yield calculation is based on the measured etch rate and predicted ion flux by using Eq. (23). It is seen that the etch yield increased up to 500 W, and remained relatively constant at higher source power (Fig. 4). The ion flux increased monotonically with increasing the source power, while the dc-bias voltage showed the reverse trend. The increase in etch yield with increasing the source power is attri-

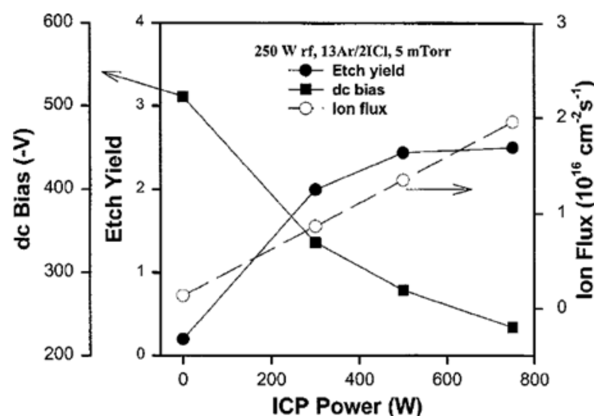

Fig. 4. Effect of ICP source power on etch yield of InN, ion flux at the sheath edge and dc bias voltage (250 W rf, 5 mTorr, 13 sccm Ar/2 sccm ICl).

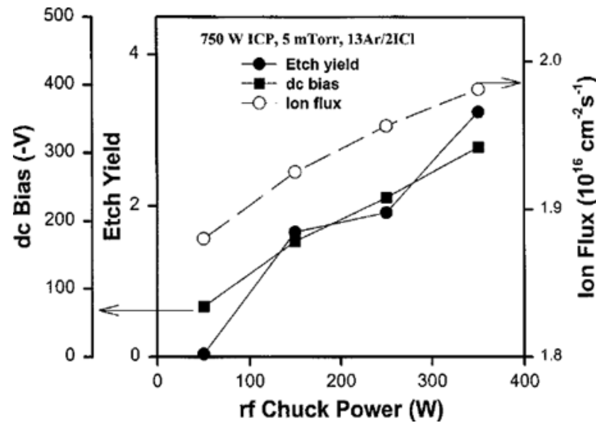

Fig. 5. Effect of rf chuck power on etch yield of InN, ion flux at the sheath edge and dc bias voltage (750 W rf, 5 mTorr, 13 sccm Ar/2 sccm ICl).

buted to the higher ion flux incident to the substrate surface and to the higher concentration of reactive species in the plasma, suggesting a reactant-limited regime. The constant etch yield with further increase of the power is mainly due to the competition between ion-assisted etch reaction and ion-assisted desorption of the reactive ions at the InN surface prior to etch reactions.

Fig. 5 shows the influence of the rf chuck power on the etch yield, ion flux and dc bias. The dc bias voltage increased monotonically with the chuck power, resulting in an increase in ion energy with the rf power, which is typical in the high density plasma systems [Hahn et al., 1999]. It is also seen that the ion flux and etch yield (or etch rate) increase with the chuck power. The increase in the etch yield with the rf power is attributed to enhanced sputter desorption of etch products as well as physical sputtering of the InN surface. The substantial increase in etch yield with increasing the chuck power also indicates that an anisotropic etching can be obtained with the increased ion bombarding energy.

The etch yield and ion flux as well as the dc biases are also affected by the reactor pressure (Fig. 6). InN showed a maximum etch yield at 15 mTorr and decreased at >15 mTorr. The increase in etch yield with pressure indicates that etching is

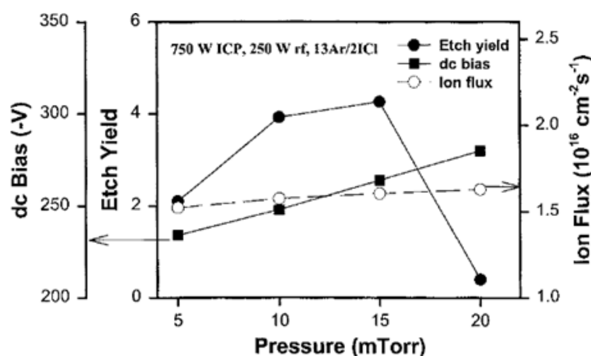

Fig. 6. Effect of pressure on etch yield of InN, ion flux at the sheath edge and dc bias voltage (750 W rf, 250 W rf, 13 sccm Ar/2 sccm ICl).

limited by mass transfer of reactive species at the lower pressures. However, as the pressure increases further, the etch yield (or the etch rate) decreases mainly due to redeposition of etch products. The higher dc-bias voltages and ion fluxes at higher pressure are attributed to increased collisional recombination.

SUMMARY AND CONCLUSIONS

Our model takes account of the effect of the rf chuck power on plasma parameters, and produces relatively accurate predictions of the plasma behavior in the ICP system. It was confirmed that the electron temperature and plasma density are mainly determined from the ion continuity and the power balance equations, respectively. The model predictions lead to the conclusion that the rf power increases not only the ion bombardment energy but also has an effect on the ion density entering the sheath layer, resulting in an increase in etch rate (or etch yield) with increasing the chuck power. The contribution of the capacitive discharge to total ion flux in the ICP etching process is less than about 6% at lower rf chuck powers. In the case of etching InN, the etch yield increased monotonically with increasing the rf chuck power, and was substantially affected by the ICP source power and pressure. The ion flux increased monotonically with increasing the source power, while the dc-bias voltage showed the reverse trend.

ACKNOWLEDGEMENTS

This work was supported by the KOSEF through the Semiconductor Physics Research Center (SPRC) at Chonbuk National University.

REFERENCES

Cho, H., Hahn, Y. B., Hays, D. C., Abernathy, C. R., Donovan, S. M. and Mackenzie, J. D., "III-Nitride Dry Etching: Comparison of Inductively Coupled Plasma Chemistries," and Pearton, S. J., *J. Vac. Sci. Technol. A*, **17**(4), 2202 (1999).

Cho, H., Vartuli, C. B., Donovan, S. M., Abernathy, C. R., Pearton, S. J., Shul, R. J. and Constantine, C., "Cl_2-Based Dry Etching of the AlGaInN System in Inductively Coupled Plasmas," *J. Vac. Sci. Technol. A*, **16**, 1631 (1998).

Collision, W. and Kushner, M. J., "Conceptual Design of Advanced Inductively Coupled Plasma Etching Tools Using Computer Modeling," *Appl. Phys. Lett.*, **68**, 903 (1996).

Economou, D. J., Bartel, T. J., Wise, R. S. and Lymberopoulos, D. P., "Two-Dimensional Direct Simulation Monte Carlo (DSMC) of Reactive Neutral and Ion Flow in a High Density Plasma Reactor," *IEEE Trans. Plasma Sci.*, **23**, 581 (1995).

Hahn, Y. B., Hays, D. C., Cho, H., Jung, K. B., Abernathy, C. R. and Pearton, S. J., "Effect of Inert Gas Additive Species on Cl_2 High Density Plasma Etching of Compound Semiconductors: Part I. GaAs and GaSb," *Appl. Surf. Sci.*, **147**, 207 (1999).

Hahn, Y. B., Hays, D. C., Cho, H., Jung, K. B., Abernathy, C. R. and Pearton, S. J., "Effect of Inert Gas Additive Species on Cl_2 High Density Plasma Etching of Compound Semiconductors: Part II. InP, InSb, InGaP and InGaAs," *Appl. Surf. Sci.*, **147**, 215 (1999).

Hahn, Y. B., Hays, D. C., Donovan, S. M., Abernathy, C. R., Han, J., Shul, R. J., Cho, H., Jung, K. B. and Pearton, S. J., "Reactive Ion Beam Etching of GaAs and Related Compounds in an Inductively Coupled Plasma of Cl_2-Ar Mixture," *J. Vac. Sci. Technol. A*, **17**(3), 763 (1999).

Hahn, Y. B., Lee., J. W., Vawter, G. A., Shul, R. J., Abernathy, C. R., Hays, D. C., Lambers, E. S. and Pearton, S. J., "Effect of Additive Noble Gases in Chlorine-Based Inductively Coupled Plasma Etching of GaN, InN and AlN," *J. Vac. Sci. Technol. B*, **17**(2), 366 (1999).

Kortshagen, U., Pukropski, I. and Tsendin, L. D., "Experimental Investigation and Fast Two-Dimensional Self-Consistent Kinetic Modeling of a Low-Pressure Inductively Coupled rf Discharge," *Physical Review E*, **51**, 6063 (1995).

Lieberman, M. A. and Gottscho, R. A., in "Physics of Thin Films," ed. by Francombe, M. and Vossen, J., Academic Press, N. Y. (1993).

Lieberman, M. A. and Lichtenberg, A. J., "Principles of Plasma Discharges and Materials Processing," John-Wiley and Sons, Inc., N. Y. (1994).

Pearton, S. J., Abernathy, C. R. and Ren, F., "Low Bias Plasma Etching of GaN, AlN and InN," *Appl. Phys. Lett.*, **64**, 2294 (1994).

Rauf, S. and Kushner, M. J., "Model for Noncollisional Heating in Inductively Coupled Plasma Processing Sources," *J. Appl. Phys.*, **81**, 5966 (1997).

Shul, R. J., in "GaN and Related Materials," ed. S. J. Pearton, Gordon and Breach, N. Y. (1997).

Shul, R. J., Briggs, R. D., Pearton, S. J., Vartuli, C. B., Abernathy, C. R., Lee, J. W., Constantine, C. and Barratt, C., "Etching of Ga-Based III-V Semiconductors in Inductively Coupled Ar and CH_4/H_2-Based Plasma Chemistries," *Mat. Res. Soc. Symp. Proc.*, **449**, 969 (1997).

Shul, R. J., McClellan, G. B., Casalnuovo, S. A., Rieger, D. J., Pearton, S. J., Constantine, C., Barrat, C., Karlicek, R. F. Jr., Tran, C. and Schurman, M., "Inductively Coupled Plasma Etching of GaN," *Appl. Phys. Lett.*, **69**, 1119 (1996).

Stewart, R. J., Vitello, P. and Graves, D. B., "Two Dimensional Fluid Model of High Density Inductively Coupled Plasma Sources," *J. Vac. Sci. Technol. B*, **12**, 478 (1994).

Wu, H.-M., Yu, B. W., Krishnan, A., Li, M., Yang, Y., Yan, J.-P. and Yuan, D.-P., "Two-Dimension Fluid Model Simulation of Bell Jar Top Inductively Coupled Plasma," *IEEE Trans. Plasma Sci.*, **25**, 776 (1997).